

# Antifungal activity of *Moringa oleifera*-based nanoemulsions against *Botrytis cinerea* in tomato

Tijjani Ahmadu<sup>a,b</sup>, Abdulaziz Bashir Kutawa<sup>a,c</sup>, Khairulmazmi Ahmad<sup>a,d</sup>, Siti Izera Ismail<sup>a</sup>, and Dzolkifli Omar<sup>a</sup>

<sup>a</sup>Department of Plant Protection, Faculty of Agriculture, Universiti Putra Malaysia, Serdang, Selangor, Malaysia <sup>b</sup>Department of Crop Production, Faculty of Agriculture and Agricultural Technology, Abubakar Tafawa Balewa University, Bauchi, Bauchi State, Nigeria <sup>c</sup>Department of Plant Science & Biotechnology, Faculty of Life Science, Federal University Dutsin-Ma, Dutsin-Ma, Katsina State, Nigeria <sup>d</sup>Institute of Plantation Studies, Universiti Putra Malaysia, Serdang, Selangor, Malaysia

## 1 Introduction

The quantity of valuable active ingredients extracted from medicinal plants needs to be reserved, improved, and upgraded into plant-based pesticides to compete with the commercial synthetic pesticides on the market. The potency of these plants has been confirmed mostly through in vitro bioassays; it has not been assessed in vivo, and their potentialities have not been studied extensively (Stangarlin et al., 2011). Formulation of these active ingredients with the inert ingredients will ease their miscibility and enhance stability, ease handling, extend their shelf life, be safe from unattractive side effects, assist in the application, and increase their effectiveness on the target organisms (Asib et al., 2015; Mathews, 2008; Ribeiro et al., 2015). Formulation of active ingredients from natural sources (products) is correlated with a lack of or low toxicity against nontarget biodiversity, ease of use from renewable sources, total biodegradability, and economic production in comparison to compounds collected by total chemical synthesis. Emulsion is the most common commercial formulation, and currently, nanoemulsion has been introduced. Nanoemulsion formulation is a pesticide delivery

technology with high acceptable potential in the area of agrochemical companies due to the fact that it is cost-effective in that it can be prepared with as little as less than 10% concentration of surfactant (Gabal et al., 2019; Lu et al., 2017; Maali and Mosavian, 2013). Again, nanoemulsions have very good stability in storage at different temperatures ( $-10^{\circ}\text{C}$  to  $55^{\circ}\text{C}$ ). It has some excellent long-term dilution characteristics in water since it is water based and highly capable of solubilizing lipophilic and hydrophilic molecules, which leads to the utilization of minimal ingredients. Additionally, nanotechnology can carry active compounds to the desired site of action, protect them against adverse effects on the environment, and enhance their potency (Asib et al., 2015; Kutawa et al., 2021a; Ribeiro et al., 2015). Nanoemulsion consists of a liquid having a small droplet size and uniformly dispersed in another immiscible liquid. The dispersed phases usually consist of droplets or particles, having a size that ranges from 10 to 100 nm and are transparent because their droplet size is below 25% of the visible light wavelength (Mishra et al., 2014). The formulations are made up of water, oil, and surfactant mixed at appropriate concentrations or ratios (Changez et al., 2000; Gupta et al., 2005; Gutiérrez et al., 2008), and the components (oil, surfactant, and water) were selected based on their ability to mix, which is assessed by the visible transparency of the phase changes of the mixture between active compound, carrier, and surfactant, and water addition by aqueous titration (Asib et al., 2015; Shafiq et al., 2007). To establish stability in nanoemulsion formulation, different points are chosen from the isotropic point in the ternary phase diagram during the process of preparation. Thus, nanoemulsion formulations that remain in one phase were evaluated based on such physical properties that include particle size, zeta potentials, viscosity, pH, surface tension, and thermostability.

The control of plant diseases using a plant source is considered an essential and eco-friendly form of disease control. Medicinal plants like *Moringa oleifera* comprise different chemical constituents that provide a source of biological and new active molecules with antifungal efficacies (Das et al., 2010; Gurjar et al., 2012). Notwithstanding, there are partial reports about the crucial aspects of plant extract formulation and elucidation of their efficacy. Recently, nanoemulsion formulations have been prepared and their efficacy has been validated from such medicinal plants that include copaiba (*Copaifera duckei*) (Da et al., 2014), oleoresin, *Opuntia ficus-indica* (Ribeiro et al., 2015), rotenone from *Derris elliptica* (Asib et al., 2015), eucalyptus oil (Sugumar et al., 2014), *Feronia elephantum* (Veerakumar et al., 2014), and plai (*Zingiber cassumunar* Roxb.) (Surassmo et al., 2013). Nanoemulsions have some broad applications, such as in cosmetic, food, and pharmaceutical industries (Solans et al., 2005), as well as in the management of pests and diseases (Wang et al., 2007; Ziedan et al., 2022). The essence of quality control of products (pesticide) is to ensure that some effective and consistent products reach the farm from the agrochemical industry. Quality control, product registration, and product development are dependent on the characterization, profiling, and quantifying of different actives and other constituents in the formulation, which includes degradation and impurities. The study of new biopesticides is dependent on the evaluation of the formulation prepared by the incorporation of plant extracts having antifungal properties. The objective of this study was to characterize nanoemulsion formulations prepared from *M. oleifera* crude extracts and evaluate their fungicidal activity (in vitro) against *Botrytis cinerea* representative isolate (BCH07) that has been observed to be highly virulent based on the pathogenicity assay.

## 2 Materials and methods

Three surfactants (Termul 5030, Termul 1284, and Tween 20, analytical grade) purchased from Sigma-Aldrich Co. (Germany) were used in the study. Edonol SP 100 served as a carrier (oil phase), and an aqueous phase (Elga Labwater 18 $\Omega$ ) was also used as presented in Table 1. The active ingredient was the crude methanol leaf extracts from *M. oleifera* collected from Ladang two (Farm two), Universiti Putra Malaysia. The *M. oleifera* plant was identified by Dr. Shamsul Khamis in the Department of Biodiversity, Institute of Biological science, University Putra Malaysia. The voucher of the specimen (SK 3029/16) was recorded in the herbarium, Institute of Biological science, Universiti Putra Malaysia.

### 2.1 Characterization of nanoemulsion

#### 2.1.1 Phase diagram system construction

The titration procedure (Asib et al., 2015; Shafiq et al., 2007) by utilizing a three-component phase diagram system was used. Surfactants were used in single and blended forms. The blend or mixed surfactants were made in ratios (w/w) as follows: Termul 5030:Termul 1284 (50:50), Termul 5030:Tween 20, and Termul 1284:Tween 20 (70:30). The surfactant and oil ratio in the experimental mixture was prepared at ratios (w/w) of 0:10, 1:9, 2:8, 3:7, 4:6,

TABLE 1 Composition of the points selected in ternary phase diagrams without the active ingredient.

Code	Composition of inert ingredients	Ratio	Percentage (%)	Total
F1	Termul 5030/ED.SP100/water	100	25:55:20	100
F2	Termul 5030/ED.SP100/water	100	20:65:15	100
F3	Termul 1284/ED.SP100/water	100	25:60:15	100
F4	Termul 1284/ED.SP100/water	100	20:70:10	100
F5	Tween 20/ED.SP100/water	100	25:60:15	100
F6	Tween 20/ED.SP100/water	100	15:70:15	100
F7	Ter. 5030:1284/ED.SP100/water	50:50	25:60:15	100
F8	Ter. 5030:1284/ED.SP100/water	50:50	15:70:15	100
F9	Ter. 5030:1284/ED.SP100/water	50:50	20:65:15	100
F10	Ter. 5030:Tw20/ED.SP100/water	70:30	25:60:15	100
F11	Ter. 5030:Tw20/ED.SP100/water	70:30	20:65:15	100
F12	Ter. 5030:Tw20/ED.SP100/water	70:30	20:70:10	100
F13	Ter. 1284:Tw20/ED.SP100/water	70:30	20:65:15	100
F14	Ter. 1284:Tw20/ED.SP100/water	70:30	20:60:20	100
F15	Ter. 1284:Tw20/ED.SP100/water	70:30	20:70:10	100

Ter., Termul, Tw, Tween 20, and ED, Edonol.

5:5, 6:4, 7:3, 8:2, 9:1, and 10:0. The correct volume of surfactant and oil according to the ratio was allowed to stand for one minute to attain equilibrium. Five percent (5%) of *M. oleifera* leaf extract was added to each of the formulations. Finally, water is added by titration into the surfactant and oil. The mixture in which transition appeared was taken and used to figure the phase domains (i.e., isotropic, monophasic, biphasic, and/or triphasic). Every sample was evaluated visibly for emulsification in terms of stability, transparency, and clarity.

Data obtained in the experiments were utilized to construct ternary phase diagrams by the use of Chemix software (version 3.5, the United Kingdom). The percentage ratio for the surfactant, water, and oil used was marked on the ternary diagram. The points that joined together determined the isotropic point of nanoemulsion in the phase diagram system. The phase diagram system was described in accordance with their surfactant phase with Edonol SP 100 as its water and oil phase (Elga Lab water 18 $\Omega$ ). Each of the mixtures was prepared in 15-mL falcon tubes sealed instantly, vortexed, and then centrifuged for 15 mins at 3500 rpm. After that, the emulsion system stability to retain a transparent one-phase appearance at room temperature was observed (Da Costa et al., 2014; Flanagan et al., 2006; Ribeiro et al., 2015).

### **2.1.2 Stability and thermostability assessment**

For short-term stability, the prepared formulations were first centrifuged at 3500 rpm for 30 mins and kept at 25°C for 1 month (Da Costa et al., 2014; Mou et al., 2008) and were observed for phase separation. The formulations were then assessed for their capability to retain a one-phase appearance (transparent) after 1 month to determine the stability of the nanoemulsion (Asib et al., 2015; Flanagan et al., 2006).

To follow the standard of the Food and Agricultural Organization for the evaluation of products (agrochemical), to remain stable in the tropical weather condition (Asib et al., 2015; Chen et al., 2000), the synthesized formulation was to be stored at 25°C for 12 weeks and kept at 54°C for 2 weeks. The changes in the appearance of samples were visibly observed.

### **2.1.3 Particle size determination**

The protocols of Asib et al. (2015) and Da Costa et al. (2014) were used for particle size determination of the synthesized nanoemulsions. Each sample (nanoemulsion) was diluted at the ratio of 1:25 in a volumetric flask and mixed gently. Measurement of the particle size of each formulation was performed by using Malvern Instruments, the United Kingdom, with a photon correlation spectrometer (Gi et al., 1992). Each sample (1 mL) was loaded into 1 cm<sup>2</sup> cuvettes (size = 10 mm × 10 mm × 44.75 mm with screw caps) and inserted into a thermostated chamber of the measuring instrument. The sample in a cuvette was inserted manually into a basin, keeping the samples at a fixed predefined temperature. The positions of the sample cuvettes were selected by the software (Windex 5) to optimize the count rate. Each of the samples (formulation) was examined directly after preparation. The experiments were repeated four times for each sample.

### **2.1.4 Measurement of surface tension**

It was determined based on the Du Nouy ring immersing procedure by using a Kruss K6 tensiometer (Kruss, the United Kingdom) connected to a platinum plate. The measurement was conducted by following the eight steps for surface tension measurement. Earlier to

measurement, the calibration was done by using double distilled H<sub>2</sub>O having a surface tension of 70.2 mN/m. Each sample of nanoemulsion (20 mL) was filled into the test vessel, and the vessel was placed on the sample table. The table was elevated by turning the screw until the ring was submerged into the sample to about 5 mm. The hand wheel was slowly turned, and the lamella formed was monitored at the sample surface. The surface tension was taken as the maximum force needed to break the film in the air when the lamella was about to break and the contact angle between the ring and the sample surface was equal to zero. The time needed to attain equilibrium was allowed until no significant change was observed. The ring was washed using methanol and flamed prior to the next measurement. Each of the runs was carried out repeatedly three times. All the measurements were conducted at room temperature.

### **2.1.5 Measurement of viscosity**

Rotational viscometer RheolabQC (Anton Paar GmbH, the United States) was utilized to measure the viscosity of the nanoemulsions without dilution. About 20 mL of the stock nanoemulsion was filled in the cup of the viscometer, tightened back, and run to measure the sample. The measurements were taken in triplicates for each sample (formulation). The cup was thoroughly washed with distilled water between samples to avoid contamination.

### **2.1.6 Zeta potentials**

The formulations were diluted using deionized H<sub>2</sub>O at the ratio (1:25) before measurement. The existing surface charges (zeta potentials) in the samples were determined by using Malvern Instruments, the United Kingdom, by laser Doppler electrophoresis. After dilution, the formulations were injected into the capillary cell. Zeta potential value gives information on the repulsive force of different compounds in the nanoformulation.

### **2.1.7 Determination of pH**

The methods of [Ribeiro et al. \(2015\)](#) and [Oliveira et al. \(2011\)](#) were used for pH determination of the synthesized nanoemulsion formulations. Exactly 9 mL of distilled water and 1 mL of nanoemulsion were transferred in a falcon tube and mixed; then the pH values were determined by insertion of the electrode into the solution for each sample three times at 25°C using a Delta 320 pH meter (Mettler Toledo, Switzerland).

### **2.1.8 Structural analysis of nanoemulsions**

The structure of the synthesized nanoemulsions was investigated using a field emission transmission electron microscopy (TEM) model (JEOL-JEMP-2100F, Tokyo, Japan). The preparation of the formulations for TEM was performed using the procedure of [Da Costa et al. \(2014\)](#) and [Goh et al. \(2015\)](#). Firstly, the sample was diluted with double distilled H<sub>2</sub>O at the ratio of 1:15 (v/v), then dropped to 200 mesh Formvar carbon-coated copper grids and stained with uranyl acetate for 3 min at 25°C. Whatman's filter paper was used to draw off the moisture, and the diluted samples were left to dry at 25°C before observing under TEM. Finally, the samples were viewed with a field emission TEM (JEOL-JEMP-2100F, Tokyo, Japan) at IBS, Universiti Putra Malaysia (UPM).

## 2.2 Fungal isolate, culture conditions, and spore preparation

Tomato fruit sample with disease symptoms (grey mold disease) was collected from glass-house in Pahang and Cameron Highlands for isolation of the pathogen. Tissue fragments (~5mm) were taken from the margin of the diseased fruit, surface sterilized with sodium hypochlorite (10%) for a period of 1 min, rinsed three times with double distilled H<sub>2</sub>O, and then placed on PDA (Difco, Becton, United States) plates amended with 1 mg/mL streptomycin to suppress the bacterial growth and incubated at 28 ± 2°C under normal fluorescent light for 3–5 days. *Botrytis cinerea* isolate was subcultured from hyphal tips until the pure culture of the isolate was obtained (Kutawa et al., 2021b). The pure culture of the *Botrytis cinerea* isolate was maintained on PDA slants and 15% glycerol stocks and stored at –20°C for further studies. The identity of these isolates (*Botrytis cinerea*) was confirmed in term of the analysis of glyceraldehyde-3-phosphate dehydrogenase (GAPDH) and internal transcribed spacer (ITS) sequence regions. BLAST searches of the obtained sequences were performed in the database of the National Centre for Biotechnology Information (NCBI) for all the isolates (Abdulaziz et al., 2017; Hossain et al., 2021). The identified isolate (BCH07) with GenBank Accession No. KU992698 for ITS and KY201460 for GAPDH showed 100% homology with *Botrytis cinerea* isolates (KP151609 for ITS and CP009819 for GAPDH), respectively. The conidial suspension was prepared by dislodging the mycelia mat of a 7-day-old culture of the fungal isolate grown on PDA, with 10–15 mL of sterilized distilled water using a sterile spatula to gently scrape the surface, and the resulting suspension was filtered by using a double-layered muslin cloth to remove the mycelium. The desired conidial suspension concentration (10 conidia/mL) was obtained by using a hemocytometer (Abd-Alla and Haggag, 2010).

## 2.3 In vitro evaluation of the nanoemulsion formulations on spore germination of *Botrytis cinerea*

Different evaluation techniques were used to determine and confirm the antifungal efficacy of the developed nanoemulsion formulations in vitro against the mycelial growth and conidial germination inhibition of *Botrytis cinerea*. The techniques used to determine percentage spore germination were broth microdilution technique, cavity slide technique, and poisoned food technique. For mycelial growth inhibition, poisoned food technique was used.

### 2.3.1 Broth microdilution technique

The method of Broekaert et al. (1990) was utilized to study the fungicidal efficacy of the fifteen developed nanoemulsion formulations in vitro against the spore germination of *Botrytis cinerea* using the microtiter plate (96 wells) or broth microdilution method (Fig. 1). Potato dextrose broth (PDB, Difco, the United States) was prepared to determine the percentage of spore germination. Fifteen different nanoemulsion formulations were screened along with Benomyl 50 WP (0.5 mg/mL) as a positive control. Each well contained 100 µL of PDB, 50 µL of stock nanoemulsion formulations, and 40 µL of conidial suspension (1 × 10<sup>6</sup> conidial concentration mL<sup>-1</sup>). For positive control, 50 µL of Benomyl 50 WP (0.5 mg/mL) was pipetted and 50 µL of methanol was used as a negative control. The treatments were in three replicates and arranged based on CRD. These Petri dishes were stored at 25°C for 24h (Lourens et al.,



FIG. 1 Microtiter plate (96 well) loaded with PDB agar, nanoemulsion, and spores of *Botrytis cinerea*.

2004). The spectrophotometer (MULTI SKAN GO) was used to measure the samples at 620nm. The inhibition of growth was calculated using the formula (Broekaert et al., 1990):

$$PGI = \frac{\Delta C - \Delta T}{\Delta C} \times 100$$

where  $\Delta C$  is the absorbance of the control microculture at 620 nm;  $\Delta T$  is the absorbance of the treatment microculture at 620 nm.

### 2.3.2 Cavity slide method

To reaffirm the fungicidal efficacy of the fifteen developed nanoemulsion formulations in vitro against the spore germination of *Botrytis cinerea*, the cavity slide method described by Ganesan and Krishnaraju (1994) was used to assess the spore germination inhibition assay. With a sterilized pipette, the stock formulation containing 5%:95% (w/w) concentration of active ingredient (a.i) and inert ingredients (carrier, surfactant, and water) were aseptically transferred to different sterilized cavity slides at the rates of 20  $\mu$ L/cavity slide. Also, the same quantity of 20  $\mu$ L of spore suspension prepared previously in (6.2.2) was aseptically added to the cavity slides containing the formulations using a different sterile pipette and mixed well with a sterile inoculation needle. For the positive control, 20  $\mu$ L of Benomyl 50 WP (0.5 mg/mL) was added, and for the negative control, 20  $\mu$ L of distilled water was added using a sterile pipette and mixed well with a sterile inoculation needle, respectively.

The slides were placed on top of the glass rods inside a moist chamber made up of a Petri plate with a sterilized moist filter paper and/or sterilized tissue paper placed at the bottom of the plate to maintain optimum humidity and temperature for incubation. The slides were stored at 25°C for 24h. After 24h of incubation, lactophenol-cotton blue (LBC) was applied to stop the spore germination and viewed under a compound light microscope. By carefully touching the edges of the coverslip with the pipette tip and allowing the counting chamber to fill by capillary force, then the spores were placed in the chambers of the hemocytometer,

mounted on the stage of a light microscope, and viewed at  $400\times$  magnification to count spore germination. Experiments were conducted in triplicates, and the conidial germination was evaluated based on the presence of a germ tube. The result was presented based on the percentage of germinated conidia in comparison to the control. The percentage of conidial germination inhibition was computed based on the formula:

$$\text{PSGI} = \frac{(\text{SC} - \text{ST})}{\text{SC}} \times 100$$

where SC is the average number of germinated conidia in control; ST is the average number of germinated conidia in the tested samples (Gameda et al., 2014).

### 2.3.3 Poisoned food technique

Potato dextrose agar (PDA, Difco, United States) was used to evaluate the fungicidal efficacy of the developed nanoemulsion formulations. Around 15 mL of PDA was transferred to each Petri plate and 0.5 mL of each formulation was added to each plate before solidification of the medium, then followed by mixing gently for uniform miscibility of the formulation and agar. The mixture was allowed to solidify and formed agar gels (Fig. 2A). Positive control Petri plates were treated with 0.5 mL of Benomyl 50WP (0.5 mg/mL), whereas the control contained only PDA (Fig. 2B). About  $100\mu\text{L}$  of the conidial suspension ( $1 \times 10^6$  conidial concentration  $\text{mL}^{-1}$ ) was spread on the prepared Petri plates each (both treated and controls). The Petri dishes were stored at  $25^\circ\text{C}$  for 5 days. The experiment was conducted in triplicates after the storage period; the conidial germination was evaluated based on the presence of a germ tube. The result was presented based on the percentage of germinated conidia in comparison to the control. The percentage of conidial germination inhibition was computed based on the following formula:

$$\text{PSGI} = \frac{(\text{SC} - \text{ST})}{\text{SC}} \times 100$$

where SC is the average number of germinated conidia in control; ST is the average number of germinated conidia in the tested samples (Gameda et al., 2014).

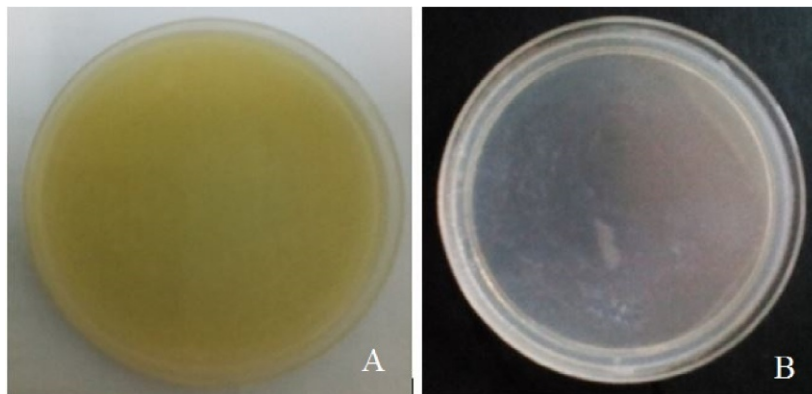


FIG. 2 (A) Potato dextrose agar (PDA) incorporated with the developed nanoemulsion formulations and (B) untreated potato dextrose agar (PDA) as a negative control.

## 2.4 In vitro assessment of the formulations on the growth of *Botrytis cinerea* mycelia

### 2.4.1 Poisoned food technique

The Petri plates were prepared as described earlier. Then the 5-day-old culture of *Botrytis cinerea* (BCH02) fungal isolate was cut (6 mm diameter) using a cork borer and the mycelial disc was transferred to the center of the plates that contained the PDA. Lines were drawn below the Petri dish for the accuracy of the measurements. The Petri dishes were stored at 25°C for 5–7 days until the Petri dish for the control was grown fully, and the colony diameter was measured daily. The inhibition of radial growth was assessed by measuring the plates with nanoemulsion formulations and Benomyl, and Petri dishes with agar only (control) and computed based on the following formula: (Verma et al., 2010).

$$\text{PIRG} = \frac{R1 - R2}{R1} \times 100$$

where R1 is the average measurement in the control; R2 is the average measurement in the treated.

## 2.5 Effect of the formulations on *Botrytis cinerea* fungal cells

The potential effect of the prepared formulations was assessed using electron microscopy methods. The microscopy methods used were transmission electron microscopy (TEM) and scanning electron microscopy (SEM) for visual observation of fungal (*Botrytis cinerea*) response to the in situ fungicidal effects of the prepared formulations against the fungal cells (conidia and mycelium).

### 2.5.1 Scanning electron microscopy (SEM)

The SEM analysis was carried out to study the fungicidal effect of *M. oleifera* methanol extract on the structure of *Botrytis cinerea* mycelia (surface level). The *Botrytis cinerea* culture was prepared for examination based on the protocol described by Adamu et al. (2021) and Hasan et al. (2014). Initially, the sample was cut (1 cm<sup>3</sup>) using a blade at the margin of the growing fungus after being treated with *M. oleifera* extract (poisoned food technique). The sample was fixed with modified Karnovsky's fixative (Karnovsky, 1965) containing paraformaldehyde in 0.05M sodium cacodylate buffer solution (pH 7.2) and 2% (v/v) glutaraldehyde. It was then incubated overnight at 4°C, the sample was rinsed with 0.1 m sodium cacodylate buffer in three changes at the interval of 30 min, the samples were then postfixed in 1% osmium tetroxide in 0.2 M PBS for 120 min, and several graded acetones (35%, 50%, 75%, and 95%) were used to dehydrate the samples for a period of 10 min each and 100% for a period of 15 min. Then, the samples were subjected to critical point drying in carbon dioxide and coated with gold by using a sputter ion coater (5–10 nm). The samples were observed under SEM (SEM: JSM-5610LV, JOEL, Japan) at the Microscopy Unit, IBS, UPM.

### 2.5.2 Transmission electron microscopy (TEM)

The TEM observation was conducted to confirm the findings of SEM and to determine the changes in the ultrastructures of *Botrytis cinerea* (conidia) due to exposure to MIC

concentration of the *M. oleifera* methanol extract. The sample (*Botrytis cinerea*) was prepared for examination under TEM using a method described by [Gunasena et al. \(2022\)](#) and [Sasidharan et al. \(2012\)](#). The sample was fixed with modified Karnovsky's fixative ([Karnovsky, 1965](#)) containing paraformaldehyde in a 0.05M sodium cacodylate buffer solution (pH 7.2) and 2% (v/v) glutaraldehyde. It was then incubated overnight at 4°C, the sample was rinsed with 0.1 m sodium cacodylate buffer in three changes at the interval of 30 min, the samples were then postfixated in 1% osmium tetroxide in 0.2M PBS for 120 min, and several graded acetones (35%, 50%, 75%, and 95%) were used to dehydrate the samples for a period of 10 min each and 100% for a period of 15 min. The sample was treated with resin and acetone mixture (1:1) for a period of 4h, then 3:1 for 1 day, and 100% of resin for another day. The samples were immersed in beam capsules filled with Spurr's resin. The ultrathin portions (1 µm in diameter) of the sample were cut with a glass knife by the use of an ultramicrotome. These portions were placed on copper grids and stained with Reynolds' lead citrate ([Reynolds, 1963](#)), and 2% uranyl acetate for a period of 10 min each. Lastly, the portions were examined under TEM (TEM MODEL JEM 2100 field emission electron microscope, Tokyo, Japan) in IBS, UPM.

## 2.6 Statistical analysis

The tests were carried out using CRD and replicated three times. The data obtained were analyzed using the analysis of variance (ANOVA) based on SAS software (version 9.4). Means with a significant difference were separated from Tukey's Studentized Range Test. The findings were presented as mean and standard deviation (Mean ± SD). Where applicable, T-test was utilized to determine the difference between the independent sample mean.

## 3 Results

### 3.1 Construction of ternary phase diagram system of the formulations

Six different ternary phase diagrams were plotted with the percentage of surfactant, oil, and water constituents to obtain a one-phase domain (isotropic) nanoemulsion region. Based on the findings, all the six ternary phase diagrams constructed have an isotropic region, which ranged from 34% to 46%. The isotropic points are transparent or clear liquid, which is stable within a certain period of time. It was also observed that the blend surfactants, Termul 5030 and Termul 1284 at 50:50 v/v concentration with Edonol SP 100 (carrier) and water system, gave the best system with a large nanoemulsion region from the phase diagram in comparison to other ternary phase diagrams where individual surfactants, Termul 5030, Termul 1284 and Tween 20, were used as surfactants at 100% concentration.

### 3.2 Selection of points for formulation composition

Fifteen points were virtually chosen from the isotropic regions of the six ternary phase diagrams constructed, and each point has a distinct composition of inert ingredients (Surfactant, oil, and water). The points were coded as F1, F2, F3, F4, F5, and F6 selected from

ternary phase diagrams constructed with a single surfactant system Termul 5030, Termul 1284, and Tween 20 (100%). Formulations coded F7, F8, F9, F10, F11, F12, F13, F14, and F15 were selected from ternary phase diagrams constructed with blend surfactant systems Termul 5030:Termul 1284 (50:50); Termul 5030:Tween 20 (70:30); and Termul 1284:Tween (70:30). All formulations consisted of surfactants from 15% to 25%, oil from 55% to 70%, and water from 10% to 20%, respectively (Table 1). The points were also selected based on the fact that they are easily miscible with the methanol leaf extract of *M. oleifera* and kept stable with one phase.

### 3.3 Stability and thermostability

Different formulations were observed for phase separation and homogeneity after accelerated centrifugation at 25°C for a period of 15 min at 3500 rpm. The results indicated that periodical observation of up to one month yielded nanoemulsion formulations with one phase, homogenous, without creaming, and colloidal formation. All formulations remained stable for a long period of storage (Table 2). The result of the exposure of the formulations to different temperatures was presented in Table 2. All formulations were stable at the temperature of 25°C after three months and for one month at 54°C. All were stable and therefore subjected to further characterization (i.e., particle size, surface tension, viscosity, zeta potentials, and pH).

TABLE 2 Stability of nanoformulations after mixing active ingredients with inert materials.

Formulation	Composition (% w/w)				Centrifugation	Stability (25°C)	Thermostability (54°C)
	MLE	S	C	H <sub>2</sub> O			
F1	5.0	23.75	52.25	19.0	√	√	√
F2	5.0	19.0	61.75	14.25	√	√	√
F3	5.0	23.75	57.0	14.25	√	√	√
F4	5.0	19.0	66.5	9.5	√	√	√
F5	5.0	23.75	57.0	14.25	√	√	√
F6	5.0	14.25	66.5	14.25	√	√	√
F7	5.0	23.75	57.0	14.25	√	√	√
F8	5.0	14.25	66.5	14.25	√	√	√
F9	5.0	19.0	61.75	14.25	√	√	√
F10	5.0	23.75	57.0	14.25	√	√	√
F11	5.0	19.0	61.75	14.25	√	√	√
F12	5.0	19.0	66.5	9.5	√	√	√

Continued

TABLE 2 Stability of nanoformulations after mixing active ingredients with inert materials—cont'd

Formulation	Composition (% w/w)				Centrifugation	Stability (25°C)	Thermostability (54°C)
	MLE	S	C	H <sub>2</sub> O			
F13	5.0	19.0	61.75	14.25	√	√	√
F14	5.0	19.0	57.0	19.0	√	√	√
F15	5.0	19.0	66.5	9.5	√	√	√

MLE, *Moringa leaf extract*; S, *surfactant*; C, *carrier (oil)*; H<sub>2</sub>O and √, *stable without phase separation*.

### 3.4 Particle size

The mean particle sizes of the nanoemulsions ranged from 53.84 to 97.14 nm (Table 3). The lowest particle size of nanoemulsion was the most desirable quality for the best formulation, and it was observed in F2 (53.84 nm), followed by F3 (63.86 nm) and F1 (67.63 nm). However, the largest particle size in the formulation was observed in F14 (97.14 nm). Based on the result of the particle size, the best formulation was F2 (53.84 nm).

TABLE 3 Characterization of the nanoemulsion formulations.

Formulation	Physical properties ( <i>n</i> = 3)					
	Particle size (nm)	Polidispersity index (PDI)	Surface tension (mN/m)	Viscosity (mPa s)	Zeta potentials (mV)	pH
	Mean ± SD	Mean ± SD	Mean ± SD	Mean ± SD	Mean ± SD	Mean ± SD
F1	67.63 ± 0.12 <sup>bc</sup>	0.375 ± 0.008	29.29 ± 0.04 <sup>defg</sup>	49.5 ± 0.2 <sup>h</sup>	20.4 ± 0.7 <sup>ab</sup>	5.62 ± 0.04 <sup>abcde</sup>
F2	53.84 ± 0.10 <sup>a</sup>	0.376 ± 0.002	29.26 ± 0.02 <sup>cdefg</sup>	30.6 ± 0.0 <sup>d</sup>	18.2 ± 0.3 <sup>a</sup>	5.45 ± 0.04 <sup>ab</sup>
F3	63.86 ± 0.35 <sup>ab</sup>	0.343 ± 0.039	29.64 ± 0.01 <sup>h</sup>	35.4 ± 0.6 <sup>f</sup>	22.3 ± 1.7 <sup>abc</sup>	5.88 ± 0.11 <sup>de</sup>
F4	70.86 ± 0.05 <sup>bc</sup>	0.185 ± 0.010	29.59 ± 0.02 <sup>h</sup>	29.7 ± 0.1 <sup>d</sup>	21.3 ± 2.3 <sup>ab</sup>	5.98 ± 0.10 <sup>e</sup>
F5	95.71 ± 0.74 <sup>ef</sup>	0.415 ± 0.023	29.05 ± 0.05 <sup>ab</sup>	33.2 ± 0.4 <sup>e</sup>	25.5 ± 0.2 <sup>bcd</sup>	5.60 ± 0.11 <sup>abcde</sup>
F6	91.70 ± 0.01 <sup>ef</sup>	0.207 ± 0.009	28.94 ± 0.04 <sup>a</sup>	24.8 ± 0.0 <sup>b</sup>	19.4 ± 1.0 <sup>a</sup>	5.74 ± 0.02 <sup>bcde</sup>
F7	76.69 ± 0.17 <sup>cd</sup>	0.309 ± 0.003	29.12 ± 0.00 <sup>bc</sup>	40.2 ± 0.4 <sup>g</sup>	30.7 ± 3.1 <sup>de</sup>	5.62 ± 0.04 <sup>abcde</sup>
F8	86.42 ± 0.24 <sup>def</sup>	0.215 ± 0.004	29.24 ± 0.01 <sup>cdef</sup>	55.8 ± 0.0 <sup>i</sup>	31.5 ± 2.1 <sup>e</sup>	5.53 ± 0.01 <sup>abc</sup>
F9	90.68 ± 7.54 <sup>ef</sup>	0.263 ± 0.003	29.31 ± 0.01 <sup>defg</sup>	32.7 ± 0.0 <sup>e</sup>	30.7 ± 2.2 <sup>de</sup>	5.77 ± 0.09 <sup>cde</sup>
F10	86.25 ± 0.33 <sup>de</sup>	0.171 ± 0.008	29.36 ± 0.02 <sup>efg</sup>	29.5 ± 0.2 <sup>d</sup>	30.4 ± 0.1 <sup>de</sup>	5.40 ± 0.07 <sup>a</sup>
F11	73.31 ± 0.85 <sup>bc</sup>	0.304 ± 0.001	29.30 ± 0.00 <sup>defg</sup>	32.7 ± 0.2 <sup>e</sup>	26.8 ± 1.4 <sup>cde</sup>	5.50 ± 0.21 <sup>abc</sup>
F12	78.15 ± 0.60 <sup>cd</sup>	0.255 ± 0.001	29.23 ± 0.01 <sup>cde</sup>	19.0 ± 0.1 <sup>a</sup>	29.8 ± 2.9 <sup>de</sup>	5.58 ± 0.16 <sup>abcd</sup>
F13	76.49 ± 1.06 <sup>cd</sup>	0.108 ± 0.006	29.39 ± 0.02 <sup>fg</sup>	26.4 ± 0.0 <sup>c</sup>	39.2 ± 1.2 <sup>f</sup>	5.48 ± 0.01 <sup>abc</sup>
F14	97.14 ± 1.23 <sup>f</sup>	0.208 ± 0.007	29.41 ± 0.02 <sup>g</sup>	58.2 ± 0.5 <sup>j</sup>	27.0 ± 1.2 <sup>cde</sup>	5.46 ± 0.10 <sup>ab</sup>
F15	93.05 ± 1.67 <sup>ef</sup>	0.147 ± 0.002	29.17 ± 0.03 <sup>bcd</sup>	35.3 ± 0.3 <sup>f</sup>	30.5 ± 0.8 <sup>de</sup>	5.58 ± 0.02 <sup>abc</sup>

Means having the same letters within each column were not significantly different at  $P \leq .05$ . Based on Tukey studentized range (HSD) test. PDI, *polidispersity index*; SD, *standard deviation*.

### 3.5 Surface tension

At the ambient temperature, the surface tension of all the selected formulations was significantly lower in comparison with one another (Table 3). It was observed that almost all formulations exhibited similar surface tension measurements. The surface tension was found in the range of 28.90–29.64 mN/m (Table 3). Formulation coded F6 was observed to have the lowest surface tension 28.90 mN/m in comparison to the other forms of the formulations. While F3 had the highest values (29.64 mN/m), based on the surface tension measurement, the formulation F6 (28.90 mN/m) was found to be the best by having the lowest surface tension.

### 3.6 Determination of viscosity

The viscosity for the formulations was studied and presented in Table 3. In general, the formulations were found to have low viscosity. The highest viscosity value (58.2 mPas) was observed in F14 formulation, whereas the lowest value (24.8 mPas) was observed in F6 formulation.

### 3.7 Zeta potentials

Values of zeta potentials fell in the range between 18.2 and 39.2 mV (Table 3). It was observed that formulations F8, F9, F10, F13, and F15 have their zeta potentials above 30.0 mV and were obtained from blend surfactants (Termul 5030:Termul 1284 (50:50), Termul 5030:Tween 20 (70:30), and Termul 1284:Tween 20 (70:30)) not from single surfactant system. Other formulations were noticed to have their zeta potentials below 30.0 mV. The highest zeta potential value (39.2 mV) was observed in F13, whereas the lowest zeta potential value (18.2 mV) was observed in F2. The higher the zeta potentials, the more stable the formulation.

### 3.8 Determination of pH

The results for pH values of the prepared nanoemulsion formulations in this study are depicted in Table 3. The findings have shown that all the formulations were moderately acidic with values that ranged from 5.40 to 5.98. Formulation F4 was observed to have the highest pH value (5.98) in comparison with formulation F10, which was observed to have the lowest pH value (5.40).

### 3.9 Structural analysis of nanoemulsions

For TEM analysis, it was conducted to determine if the particle droplets of the prepared nanoemulsions were oval in shape and the particle sizes of these formulations were in line with Malvern Zetasizer ZS. Results observed in the TEM micrographs (Fig. 3) were representatives of the prepared nanoemulsions, which showed that their particle droplets were spherical and the sizes of their particles were less than 100 nm, which were measured using TEM and are consistent with the size obtained using photon correlation spectroscopy of Malvern Zetasizer ZS (<100 nm) (Fig. 3).

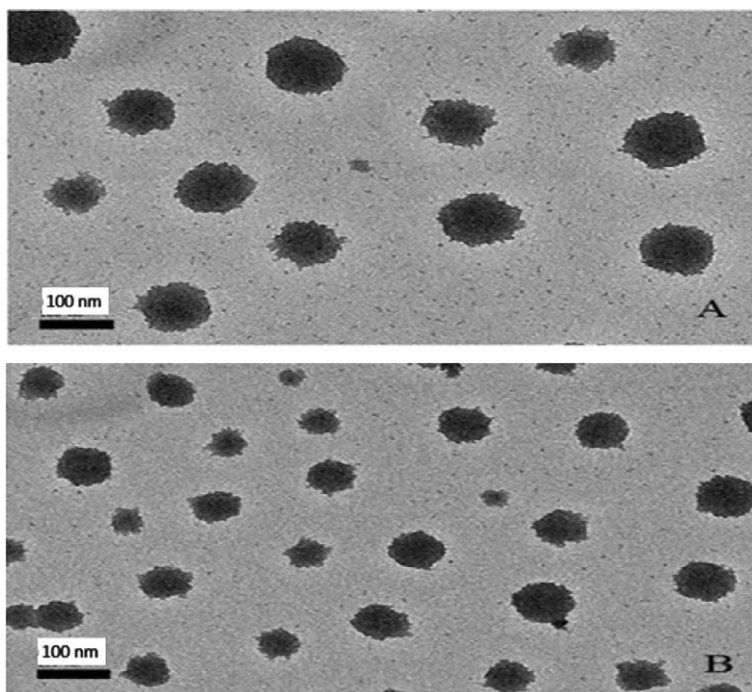


FIG. 3 TEM micrographs showing spherical particle droplets from representative nanoemulsion formulations. (A) Micrograph for spherical shapes of particle droplets from F9 and (B) micrograph spherical particle shapes of droplets from F13.

### 3.10 In vitro evaluation of the nanoemulsion formulations on spore germination of *Botrytis cinerea*

#### 3.10.1 Broth microdilution technique and cavity slide method

The effects of the developed nanoemulsion formulations on the spore germination of *Botrytis cinerea* in vitro using broth micro dilution technique and cavity slide method were depicted in Table 4. The findings have shown that the incorporation of the active ingredient (a.i) at 5% and 10% into all the developed nanoemulsion formulations inhibited spore germination of the representative isolate of *Botrytis cinerea* (BCH07) up to 100% with the exception of some formulations (F1, F2, F3, F5, F7, F8, and F11) that showed inhibition of spore germination that ranged from 98.10% to 99.60% at 5% concentration of the active ingredient. The result also showed that formulations F1, F2, F3, F5, F7, F8, and F11 were comparable to the standard control Benomyl 50 WP (0.5 mg/mL) that gave 98.66% and 98.87% spore germination inhibition values. Furthermore, the results on the effects of the formulation on the spore germination of the fungus (100%) also in vitro using cavity slide method confirmed the results of broth microdilution technique (Table 4). The control (untreated) showed 0% spore germination inhibition under both techniques of in vitro evaluation.

**TABLE 4** In vitro effects of nanoemulsion formulations on spore germination and mycelial growth of *Botrytis cinerea* using broth microdilution and cavity slide methods.

Formulation code	Broth microdilution (%)		Cavity slide (%)	
	5% (a.i)	10% (a.i)	5% (a.i)	10% (a.i)
F1	98.50	100	100	100
F2	98.33	100	100	100
F3	98.74	100	100	100
F4	100	100	100	100
F5	99.00	100	100	100
F6	100	100	100	100
F7	99.60	100	100	100
F8	98.25	100	100	100
F9	100	100	100	100
F10	100	100	100	100
F11	98.10	100	100	100
F12	100	100	100	100
F13	100	100	100	100
F14	100	100	100	100
F15	100	100	100	100
Standard control (Benomyl 50WP 0.5mg/mL)	98.66	98.87	100	100
Negative control	0	0	0	0

a.i, active ingredient.

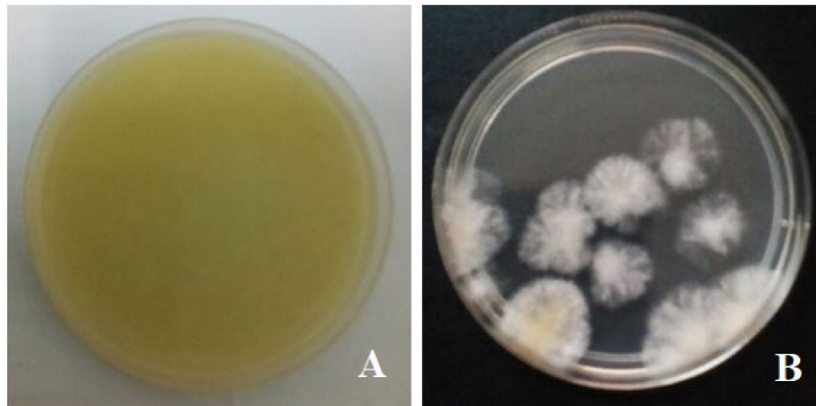
### 3.10.2 Poisoned food technique

Table 5 presents the results of the effects of the developed nanoemulsion formulations on the inhibition of spore germination and radial mycelial growth of *Botrytis cinerea* based on the poisoned medium technique (in vitro). The findings were depicted as mean  $\pm$  standard deviation. Results indicated that all formulations inhibited spore germination and radial mycelial growth (Fig. 4A) of the representative fungus (isolate BCH07) in comparison to the control with 0% inhibition (Fig. 4B). The result also showed 100% PIRG by F12, F13, F14, F15, F7, F8, F9, and F10 at both 5% and 10% active ingredient concentration in the formulations and 100% PISG at 10% by F13 and F14 formulations. This showed that there is no statistical difference ( $P \leq .05$ ) among these formulations on PIRG at both concentrations (5% and 10%). The results indicated that other formulations showed variations in their inhibition of spore germination and mycelial growth at both concentrations with F1 to F15 having PIRG that ranges from 97.99 to 99.66 at 5% concentration, while F1 to F12 and F15 having PIRG that ranges from 98.65 to 99.66 at 10% concentration, respectively.

**TABLE 5** Effect of nanoemulsion formulations on *Botrytis cinerea* spore germination and mycelial growth in vitro using poisoned food method.

Formulation code	PS GI (%)		PIRG (%)	
	5% (a.i) Means $\pm$ SD	10% (a.i) Means $\pm$ SD	5% (a.i) Means $\pm$ SD	10% (a.i) Means $\pm$ SD
F1	98.63 $\pm$ 1.59 <sup>ab</sup>	98.99 $\pm$ 0.99 <sup>ab</sup>	98.41 $\pm$ 1.74 <sup>ab</sup>	99.60 $\pm$ 0.69 <sup>a</sup>
F2	98.33 $\pm$ 1.15 <sup>ab</sup>	98.99 $\pm$ 1.72 <sup>ab</sup>	98.41 $\pm$ 1.37 <sup>ab</sup>	98.80 $\pm$ 1.19 <sup>ab</sup>
F3	98.00 $\pm$ 0.01 <sup>ab</sup>	98.98 $\pm$ 1.00 <sup>ab</sup>	99.20 $\pm$ 1.37 <sup>ab</sup>	100 $\pm$ 0.00 <sup>a</sup>
F4	98.66 $\pm$ 1.64 <sup>ab</sup>	99.60 $\pm$ 1.15 <sup>a</sup>	98.81 $\pm$ 2.06 <sup>ab</sup>	99.60 $\pm$ 0.69 <sup>a</sup>
F5	97.99 $\pm$ 0.53 <sup>ab</sup>	98.66 $\pm$ 0.67 <sup>ab</sup>	99.20 $\pm$ 1.37 <sup>ab</sup>	100 $\pm$ 0.00 <sup>a</sup>
F6	97.99 $\pm$ 0.99 <sup>ab</sup>	98.65 $\pm$ 1.17 <sup>ab</sup>	98.41 $\pm$ 1.37 <sup>ab</sup>	100 $\pm$ 0.00 <sup>a</sup>
F7	99.33 $\pm$ 0.57 <sup>ab</sup>	99.66 $\pm$ 0.58 <sup>a</sup>	100 $\pm$ 0.00 <sup>a</sup>	100 $\pm$ 0.00 <sup>a</sup>
F8	99.66 $\pm$ 0.57 <sup>a</sup>	99.66 $\pm$ 0.57 <sup>a</sup>	100 $\pm$ 0.00 <sup>a</sup>	100 $\pm$ 0.00 <sup>a</sup>
F9	99.32 $\pm$ 0.58 <sup>ab</sup>	99.66 $\pm$ 0.58 <sup>a</sup>	100 $\pm$ 0.00 <sup>a</sup>	100 $\pm$ 0.00 <sup>a</sup>
F10	98.66 $\pm$ 0.57 <sup>ab</sup>	99.00 $\pm$ 1.00 <sup>ab</sup>	100 $\pm$ 0.00 <sup>a</sup>	100 $\pm$ 0.00 <sup>a</sup>
F11	99.32 $\pm$ 1.15 <sup>ab</sup>	99.33 $\pm$ 0.58 <sup>ab</sup>	98.81 $\pm$ 2.06 <sup>ab</sup>	99.60 $\pm$ 0.69 <sup>a</sup>
F12	99.66 $\pm$ 0.57 <sup>a</sup>	99.66 $\pm$ 0.57 <sup>a</sup>	100 $\pm$ 0.00 <sup>a</sup>	100 $\pm$ 0.00 <sup>a</sup>
F13	99.66 $\pm$ 0.55 <sup>a</sup>	100 $\pm$ 0.00 <sup>a</sup>	100 $\pm$ 0.00 <sup>a</sup>	100 $\pm$ 0.00 <sup>a</sup>
F14	99.66 $\pm$ 0.57 <sup>a</sup>	100 $\pm$ 0.00 <sup>a</sup>	100 $\pm$ 0.00 <sup>a</sup>	100 $\pm$ 0.00 <sup>a</sup>
F15	99.66 $\pm$ 0.57 <sup>a</sup>	99.66 $\pm$ 0.57 <sup>a</sup>	100 $\pm$ 0.00 <sup>a</sup>	100 $\pm$ 0.00 <sup>a</sup>
Standard control (Benomyl, 0.5 mg/mL)	98.66 $\pm$ 1.15 <sup>ab</sup>	98.87 $\pm$ 1.52 <sup>ab</sup>	98.01 $\pm$ 1.81 <sup>ab</sup>	98.80 $\pm$ 1.19 <sup>ab</sup>
Negative control	0.00 $\pm$ 0.00 <sup>c</sup>			
CV	0.96	0.98	1.29	0.64

Means (n=3) followed by the same letters within each column are not significantly different at  $P \leq .05$  according to Tukey studentized range (HSD) test. PC, positive (standard) control; CV, coefficient of variation.



**FIG. 4** (A) Potato dextrose agar (PDA) incorporated with the F13 prepared nanoemulsion formulation showing no spore germination and (B) potato dextrose agar (PDA) serving as a negative control showing spore germination of BCH07 *Botrytis cinerea* isolate.

### 3.11 Scanning electron microscope observations on *Botrytis cinerea* mycelia

Observation of the changes of *Botrytis cinerea* mycelium treated with nanoemulsion formulations incorporated with *M. oleifera* (crude extracts) through SEM micrographs showed that the formulations have an adverse effect on the mycelium in comparison to the control. The effects noticed were reduced hyphal length and diameters, lysis, shrinkage, abnormal growth, aggregation, disruption, shrinkage and aggregation, shrinkage and lysis, and the formation of pores on the mycelium (Fig. 5). The control micrographs for mycelium were observed with smooth surfaces and normal growth.

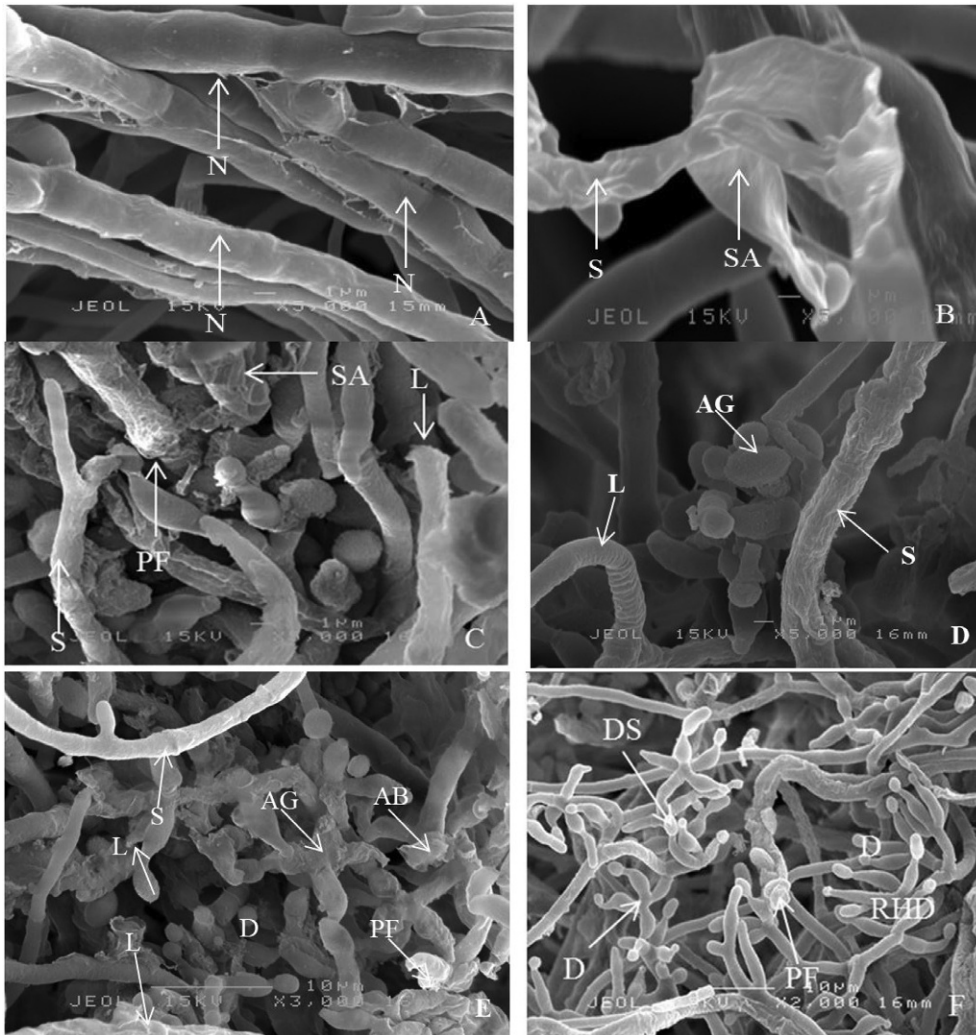


**FIG. 5** SEM micrographs showing the effects of formulations from *M. oleifera* extract on the mycelium of *Botrytis cinerea* (BCH07). (A) Control, (B) shrinkage and aggregation on the treated mycelia, (C) lysis and pore formation, (D) shrinkage, lysis, and aggregation, (E) disruption and abnormal growth, and (F) reduced hyphal diameters and length, formation of pore and disruption. Letters in the micrograph: N, normal; L, lysis; S, shrinkage; D, disruption; AG, abnormal growth; PF, pore formation; RHD, reduced hyphal length and diameters; SA, shrinkage and aggregation.

### 3.12 Transmission electron microscope observations on *Botrytis cinerea* cells

The results of TEM are indicated in Fig. 6. The results revealed that the untreated conidia (controls) grew with normal ultrastructural components. The micrographs of TEM for the control conidia have a normal cell wall (300–400nm) with a two-layer structure, cytoplasm

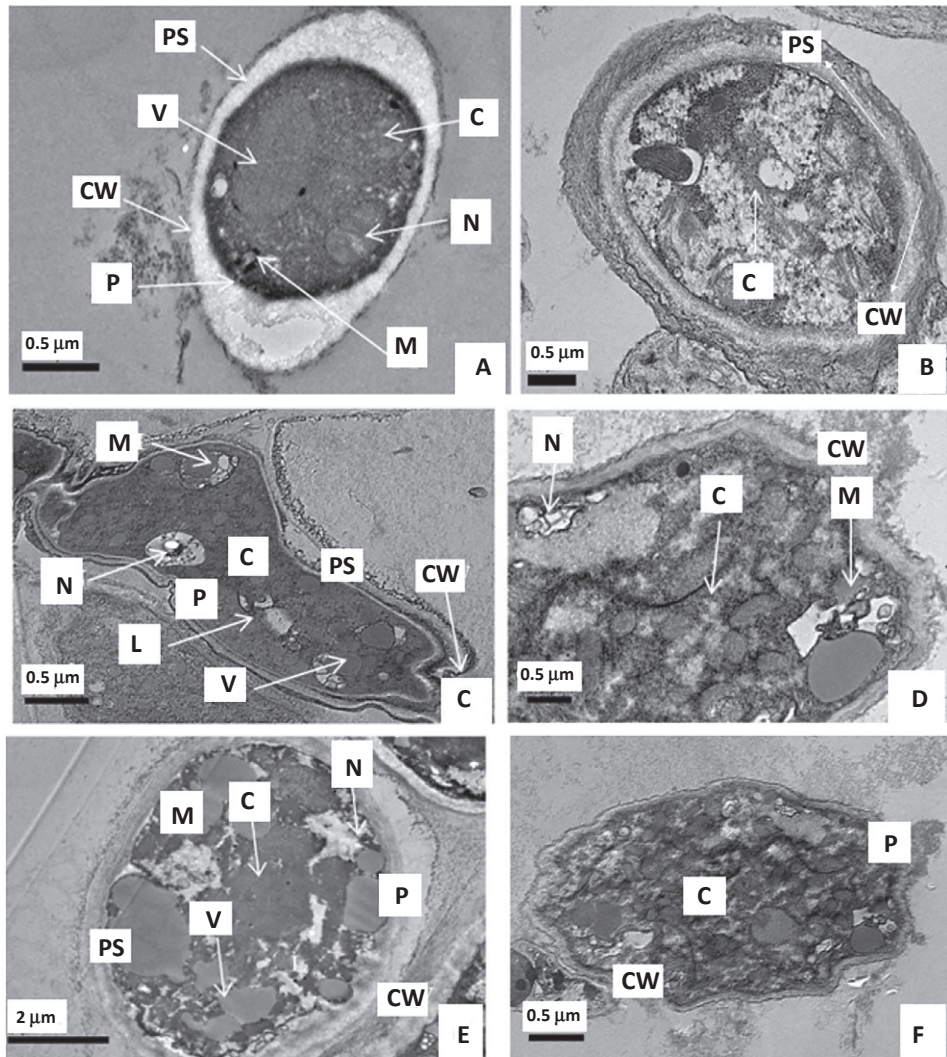


**FIG. 6** Transmission electron micrographs showing the effect of formulations on cross-section *Botrytis cinerea* conidia (BCH07). (A) Control, (B) pore formation and disruption of organelles, (C) vacuolation and disruption of organelles, (D) disruption of organelles, (E) disruption of organelles and cell wall, and (F) cell wall degradation after exposure to the formulation. Letters in the micrograph: C, cytoplasm; CW, cell wall; P, plasmalemma; PS, periplasmic space; M, mitochondria; N, nucleus; V, vacuole; L, lysosome.

matrix (cytosol) with nucleolus and nucleus, plasmalemma, vacuole, mitochondria, lipids, etc. An external covering of the cell wall was found to be electron dense and thin; a thick inner wall was less and uniformly electron dense. Where the plasma membrane was tightly attached to the wall of the cell, the cytoplasm matrix was found dispersed throughout the cell, and the shape of the nucleus was oval. Mitochondria were many, had an average electron density, and are ovoid in shape. Glycogen and lipids were the major intracellular nutrient reserves. Unlike the control, the micrographs for the spores that were treated have shown that the nanoemulsion formulations at a 5% concentration of active ingredients caused irreversible changes in the ultrastructure of the *Botrytis cinerea* conidia. The micrographs have also shown that there was precipitation of the cytoplasm and disruption of cellular organelles. In addition, the cell wall had shrunk and was more permeable with an irregular shape. The cell membrane was almost destroyed or found not attached to the wall of the cell. Moreover, a small periplasmic space was observed between the cell wall and the cytoplasm.

## 4 Discussion

Due to the negative effect that is associated with the usage of synthetic pesticides to manage diseases of plants, this led researchers to put much emphasis on the formulation of plant-based biopesticides, because of the need to develop a reliable and promising solution for plant disease management that is safe for the environment and humans (Amadioha, 2002; Taiga et al., 2008). Progress in biopesticide development at the commercial level has been substantial. Aspire and BioSave100 and 110 were the first commercially formulated biocontrol biopesticides registered and sold by the United States Environmental Protection Agency (US EPA). In this regard, active compounds from medicinal plants such as *M. oleifera* need to have an effective delivery technology that extends their shelf life and increases efficacy as well as stability under commercial situations. The advent of nanotechnology contributes a lot in the area of agricultural plant protection by giving rise to stable nanoformulations that enhance the efficacy of the active compounds when compared to synthetic products. The success of any biocontrol agent in commercial use depends largely on the quality of how it is formulated to effectively compete in the market (Janisiewicz and Korsten, 2002; Nunes, 2012). Such formulations should be cost-effective (i.e., economical to produce), easy to handle, and very effective when applied to the crops (Asib et al., 2015; Janisiewicz and Korsten, 2002).

In the present study, nonionic surfactants (Termul 5030, Termul 1284, and Tween 20) that have good compatibility and relatively low toxicity and are eco-friendly, easily biodegradable, and environmentally sustainable were utilized in the plotting of the ternary phase diagram, which greatly influenced the solubility and distribution of the *M. oleifera* crude extracts (active ingredients) and the carrier (Edonol SP 100) and allowed the sufficient dispersion of the nanoformulation in water that was in accordance with the earlier works of Asib et al. (2015) and Da Costa et al. (2014). The presence of wider homogenous isotropic nanoemulsion regions in the phase diagrams was stabilized by the surfactants and was highly influenced by the properties of the surfactants (Trotta et al., 1999). In the water in oil (W/O) nanoemulsion, surfactants play a significant role in lowering both interfacial and surface tension by

accumulating at the interface of the formulations. Therefore, a surfactant is required to enhance the synthesis of the nanoemulsion and guarantee its kinetic stability for long-term storage (McClements, 2004, 2012).

Because nanoemulsions require a complex and varied structure, as well as different active ingredients, their characterization is therefore challenging. As a result, a number of tools were developed to assist in characterizing the formulation effectively; therefore, knowledge is imperative for effective commercial investigations (Bali et al., 2011). The optimized formulations selected from the existing nanoemulsion region as confirmed by plotted phase diagrams were characterized for their zeta potential, particle size, surface tension, viscosity, and pH. Additionally, centrifugation, and various stability tests were carried out on the formulations selected from the phase diagrams. Centrifugation and exposure to high temperature for some hours or days (1–14 days) were the most commonly utilized stress conditions to rapidly assess the stability of nanoemulsions after preparation (Lima et al., 2008), and all our formulations were considered stable because no flocculation, phase separation, or creaming was noticed during the study period. This has been pointed out by the reports of Komaiko and McClements (2014), Oliveira et al. (2011), and Ribeiro et al. (2015) who reported that the stability assessment is required because of its predictive ability that helped to hasten changes that may likely occur in the formulations under market conditions.

Regarding particle size measurements, the particle sizes determined in the nanoemulsion of the present study were less than 100 nm, which is based on the previous works on droplet size of nanoemulsion (Asib et al., 2015; Shafiq et al., 2007; Bali et al., 2010, 2011; Vior et al., 2011). Due to their small droplet sizes (submicrometer size), nanoemulsions have a chance to enter deep into the tissue of the target pest and efficiently convey the active ingredients to the targeted tissue effectively (Tamilvanan, 2009). The nanoemulsions with the dispersion of water and oil that are stabilized by an interracial film of surfactant compound with a droplet size below 100 nm were also reported by Kreuter et al. (1994). Due to the fact that nanoemulsions are easily produced by mixing and/or blending with a long shelf life, the nanoemulsions provide solubilization capacities like simple micelle solutions, emulsions, and suspensions and are also translucent.

In accordance with the surface tension, generally, the prepared nanoemulsions have quite, relatively similar and lower surface tension (below 30 mN/m), and in nanoemulsion, the advantage of lower surface tension is in the enhancement of wetting, penetration, and spreading of the nanoemulsion (Rao and McClements, 2012; Tadros et al., 2004). In addition, the lower surface tension values allow the particles to spread and penetrate uniformly on the target pest with a smaller contact angle at the time of application. The surface tension value below 30 mN/m also indicated the situation in which the surfactant acts in reducing the interfacial tension in the prepared formulations (Kreuter et al., 1994). With the exception of formulations F1 (49.5 mPas), F8 (55.8 mPas), and F14 (58.2 mPas), the rest of the selected nanoemulsions had low viscosity (mPas), and the low viscosity values of the nanoemulsion are vital in its preparation and application as earlier reported by Bali et al. (2011). The low viscosity of the present nanoemulsions coincides with one of the attributes of nanoemulsions (Baboota et al., 2007; Da Costa et al., 2014). In this study, 6 formulations, viz., F7 (30.7 mV), F8 (31.5 mV), F9 (30.7 mV), F10 (30.4 mV), F13 (39.2 mV), and F15 (30.5 mV), have surface charges above 30 mV. Typically, a zeta potential value that exceeded 30 mV irrespective of the negative or positive charges is regarded as stable nanoemulsion. Zeta potential is associated with the stability of colloidal

dispersion because it signifies the repulsion between neighboring like-charged molecules in dispersion (Bali et al., 2010, 2011). In nanoemulsions, charge interaction is determined by zeta potential, and particles that are very small have high zeta potential that confers their stability, that is, the dispersion or solution will obstruct aggregation. Thus, there are minimum chances of flocculation or coagulation of the nanoemulsions in the environment. The pH values of less than 6 in the prepared nanoemulsions formulations coincide with one of the characteristics of nanoemulsions (Da Costa et al., 2014). In comparison with particle size and structural morphology of nanoemulsions, TEM micrographs have confirmed that the particle sizes and shapes of the prepared nanoemulsion formulations were in conformity with those obtained from the Malvern Zetasizer ZS measurements (Da Costa et al., 2014; Goh et al., 2015).

The tested formulations have successfully inhibited the *Botrytis cinerea* mycelial and conidial growth under in vitro conditions. Hence, considering the in vitro effect of the formulations, it was evidenced that exposure of the *Botrytis cinerea* mycelium and conidia to the formulations at a 5% concentration of *M. oleifera* led to some irreversible surface and ultrastructural changes that include lysis, shrinkage, abnormal growth, pore formation, vacuolation, and cytoplasmic degeneration, etc. As a result of the disruption of the *Botrytis cinerea* fungal cell wall, the outer layer was electron dense, the cytosol and cell membrane of the fungal cell had detached from the cell wall and shrunk, and the nucleus and cellular organelles also precipitated partially or completely. This might be because of the potent active ingredients available in the leaf extract of *M. oleifera* incorporated in the formulations, which is consistent with the previous reports of Parvu et al. (2010) who documented the changes in the conidia of the *Botrytis cinerea* fungus incited by the extract of *Berberis vulgaris* plant. Similarly, Parvu et al. (2008) reported the fungicidal effect of *Chelidonium majus* extracts on *Botrytis cinerea* fungus under in vitro conditions and ultrastructural alteration was observed on the fungal spore. More so, the report of Parvu and Parvu (2011) on the fungicidal effect of *Allium obliquum*, *Allium ursinum*, *Allium fistulosum*, *Berberis vulgaris*, *Chelidonium majus*, and *Aloe vera* extracts revealed the ultrastructural changes induced by the plant extracts on the spores of *Botrytis cinerea*, *Aspergillus niger*, *Fusarium oxysporum* f. sp. *gladioli*, *Botrytis paeoniae*, *Heterosporium pruneti*, *Fusarium oxysporum* f.sp. *tulipae*, *Penicillium gladioli*, *Sclerotinia sclerotiorum*were, and *Penicillium expansum* after being visualized on the electron microscope.

---

## 5 Conclusion

---

It is well documented that plants contain natural phytochemical compounds that could be exploited as biopesticides. These compounds act as antimicrobial, antifungal, antioxidant, antibacterial, antiulcer, antiinflammatory, diuretic, and anticancer agents to mention a few. The active ingredients in these valuable medicinal plants need to be upgraded or enhanced into plant-based pesticides to compete with the commercial synthetic pesticides in the market. To ease the handling of the active ingredients, extend their shelf life, assist in the application, and increase their efficacies on the target organisms, the present research was conducted to characterize nanoemulsion formulations prepared by incorporating *M. oleifera* crude extracts and evaluate their fungicidal activity against *Botrytis cinerea* representative isolate (BCH07) in vitro. And all the developed nanoemulsion formulations have

inhibited the growth of *Botrytis cinerea* mycelia and conidia under in vitro condition. There is a need for future research to focus on many other plant species with fungicidal potentialities to protect the environment and humans from the effect of these unfriendly synthetic chemicals.

## Acknowledgments

We appreciate the effort of all the staff of Mycology Laboratory, Department of Plant Protection, UPM, for their guidance and cooperation during the execution of the work.

## Funding

The authors wish to thank the Fundamental Research Grant Schemes (FRGS), obtained from the Higher Education Ministry, Malaysia, which was used to fund this work with Grant Number UPM/700-2/1/FRGS/07-01-15-1647FR and the Universiti Putra Malaysia where the research was conducted and supervised.

## Compliance with ethical standards

All the ethics were duly followed during this work.

## Conflict of interest

The authors declared no competing interests.

## Author contributions

T.A. conducted the study and developed the first draft of the manuscript. ABK paraphrased and edited the manuscript. K.A. S.I.I., and D.O. supervised and edited the final draft of the manuscript.

## References

- Abd-Alla, M.A., Haggag, W.M., 2010. New safe methods for controlling anthracnose disease of mango (*Mangifera indica* L.) fruits caused by *Colletotrichum gloeosporioides* (Penz.). *J. Am. Sci.* 8, 361–366.
- Abdulaziz, B.K., Kamaruzaman, S., Khairulmazmi, A., Zulkifli, A.S., Mohd, S., Norzihan, A., 2017. Characterisation and pathological variability of *Exserohilum turcicum* responsible for causing northern corn leaf blight (NCLB) disease in Malaysia. *Malays. J. Microbiol.* 13 (1), 41–49.
- Adamu, A., Ahmad, K., Siddiqui, Y., Ismail, I.S., Asib, N., Bashir Kutawa, A., Berahim, Z., 2021. Ginger essential oils-loaded nanoemulsions: potential strategy to manage bacterial leaf blight disease and enhanced rice yield. *Molecules* 26 (13), 3902.
- Amadioha, A.C., 2002. Fungitoxic effects of extracts of *Azadirachta indica* against *Cochliobolus miyabeanus* causing brown spot disease of rice. *Arch. Phytopathol. Plant Prot.* 35 (1), 37–42.
- Asib, N., Omar, D., Rita, M.A., Abdullah, N.P., 2015. Preparation, characterization and toxicity of nano-emulsion formulations of rotenone extract of *Derris elliptica*. *J. Chem. Biol. Phys. Sci.* 5, 3989–3997.
- Baboota, S., Al-Azaki, A., Kohli, K., Ali, J., Dixit, N., Shakeel, F., 2007. Development and evaluation of a microemulsion formulation for transdermal delivery of terbinafine. *PDA J. Pharm. Sci. Technol.* 61, 276–285.
- Bali, V., Ali, M., Ali, J., 2010. Study of surfactant combinations and development of a novel nanoemulsion for minimising variations in bioavailability of ezetimibe. *Colloids Surf. B Biointerfaces* 76, 410–420.
- Bali, V., Ali, M., Ali, J., 2011. Nanocarrier for the enhanced bioavailability of a cardiovascular agent: in vitro, pharmacodynamic, pharmacokinetic and stability assessment. *Int. J. Pharm.* 403, 46–56.

- Broekaert, W.F., Terras, F.R., Cammue, B.P., Vanderleyden, J., 1990. An automated quantitative assay for fungal growth inhibition. *FEMS Microbiol. Lett.* 69 (1-2), 55–59.
- Changez, M., Varshney, M., Aerosol, O.T., 2000. Microemulsions as transdermal carriers of tetracaine hydrochloride. *Drug Dev. Ind. Pharm.* 26, 507–512.
- Chen, F., Wang, Y., Zheng, F., Wu, Y., Liang, W., 2000. Studies on cloud point of agrochemical microemulsions. *Colloids Surf. A: Physicochem. Eng. Asp.* 175, 257–262.
- Da Costa, S., Basri, M., Shamsudin, N., Basri, H., 2014. Stability of positively charged nanoemulsion formulation containing steroidal drug for effective transdermal application. *J. Chem.* 2014.
- Da, C.R., Rodrigues, E., Ferreira, A.M., Vilhena, J.C., Almeida, F.B., Cruz, R.A., Florentino, A.C., Fernandes, C.P., 2014. Development of a larvicidal nanoemulsion with Copaiba (*Copaifera duckei*) oleoresin. *Rev. Bras. Farmacogn.* 24, 699–705.
- Das, K., Tiwari, R.K.S., Shrivastava, D.K., 2010. Techniques for evaluation of medicinal plant products as antimicrobial agent: current methods and future trends. *J. Med. Plants Res.* 4, 104–111.
- Flanagan, J., Kortegaard, K., Pinder, D.N., Rades, T., Singh, H., 2006. Solubilisation of soybean oil in microemulsions using various surfactants. *Food Hydrocol.* 20, 253–260.
- Gabal, E., Mohamed, M.A., Abd-Elsalam, K.A., 2019. Botrytis gray mold nano-or biocontrol: present status and future prospects. *Nanobiotechnol. Appl. Plant Prot.*, 85–118.
- Ganesan, T., Krishnaraju, J., 1994. Antifungal properties of wild plants. *Adv. Plant Sci.* 7 (1), 185–187.
- Gemeda, N., Woldeamanuel, Y., Asrat, D., Debella, A., 2014. Effect of essential oils on *Aspergillus* spore germination, growth and mycotoxin production: a potential source of botanical food preservative. *Asian Pac. J. Trop. Biomed.* 4, 373–381.
- Gi, H.J., Chen, S.N., Hwang, J.S., Tien, C., Kuo, M.T., 1992. Studies of formation and interface of oil-water microemulsion. *Chin. J. Physiol.* 30, 665–678.
- Goh, P.S., Ng, M.H., Choo, Y.M., Amru, N.B., Chuah, C.H., 2015. Production of nanoemulsions from palm-based tocotrienol rich fraction by microfluidization. *Molecules* 20, 19936–19946.
- Gunasena, M.T., Rafi, A., Mohd Zobir, S.A., Hussein, M.Z., Ali, A., Kutawa, A.B., Ahmad, K., 2022. Phytochemicals profiling, antimicrobial activity and mechanism of action of essential oil extracted from ginger (*Zingiber officinale* Roscoe cv. Bentong) against *Burkholderia glumae* causative agent of bacterial panicle blight disease of rice. *Plants* 11 (11), 1466.
- Gupta, R.R., Jain, S.K., Varshney, M.A.O.T., 2005. Water-in-oil microemulsions as a penetration enhancer in transdermal drug delivery of 5-fluorouracil. *Colloids Surf. B Biointerfaces* 41, 25–32.
- Gurjar, M.S., Ali, S., Akhtar, M., Singh, K.S., 2012. Efficacy of plant extracts in plant disease management. *Agric. Sci.* 3, 425–433.
- Gutiérrez, J.M., González, C., Maestro, A., Sole, I., Pey, C.M., Nolla, J., 2008. Nano-emulsions: new applications and optimization of their preparation. *Curr. Opin. Colloid Interface Sci.* 13, 245–251.
- Hasan, S., Singh, K., Danisuddin, M., Verma, P.K., Khan, A.U., 2014. Inhibition of major virulence pathways of *Streptococcus mutans* by quercitrin and deoxynojirimycin: a synergistic approach of infection control. *PLoS One* 9, 91736.
- Hossain, M.I., Ahmad, K., Vadamalai, G., Siddiqui, Y., Saad, N., Ahmed, O.H., Kutawa, A.B., 2021. Phylogenetic analysis and genetic diversity of *Colletotrichum falcatum* isolates causing sugarcane red rot disease in Bangladesh. *Biology* 10 (9), 862.
- Janisiewicz, W.J., Korsten, L., 2002. Biological control of postharvest diseases of fruits. *Annu. Rev. Phytopathol.* 40, 411–441.
- Karnovsky, M.J., 1965. A formaldehyde-glutaraldehyde fixative of high osmolality for use in electron microscopy. *J. Cell Biol.* 27, 137–138.
- Komaiko, J., McClements, D.J., 2014. Optimization of isothermal low-energy nanoemulsion formation: hydrocarbon oil, non-ionic surfactant, and water systems. *J. Colloid Interface Sci.* 425, 59–66.
- Kreuter, J., Swarbrick, J., Boyalan, J.C., 1994. *Encyclopedia of Pharmaceutical Technology*. New York, vol. 10, pp. 165–190.
- Kutawa, A.B., Ahmad, K., Ali, A., Hussein, M.Z., Abdul Wahab, M.A., Adamu, A., Hossain, M.I., 2021a. Trends in nanotechnology and its potentialities to control plant pathogenic fungi: a review. *Biology* 10 (9), 881.
- Kutawa, A.B., Ahmad, K., Ali, A., Zobir, S.A.M., Wahab, M.A.A., 2021b. Identification and characterization of pathogen responsible for causing southern corn leaf blight (SCLB) disease in Malaysia. *Int. J. Agric. Biol.* 26, 607–616.

- Lima, C.G., Vilela, A.F.G., Silva, A.A.S., Piannovski, A.R., Silva, K.K., Carvalho, V.F.M., de Musis, C.R., Machado, S.-R.P., Ferrari, M., 2008. Desenvolvimento e avaliação da estabilidade física de emulsões O/A contendo óleo de babaçu (*Orbignya oleifera*). *Rev. Bras. Farmacogn.* 89, 239–245.
- Lourens, A.C.U., Reddy, D., Başer, K.H.C., Viljoen, A.M., Van Vuuren, S.F., 2004. *In vitro* biological activity and essential oil composition of four indigenous South African *Helichrysum* species. *J. Ethnopharmacol.* 95 (2), 253–258.
- Lu, W.C., Huang, D.W., Wang, C.C., Yeh, C.H., Tsai, J.C., Huang, Y.T., Li, P.H., 2017. Preparation, characterization, and antimicrobial activity of nanoemulsions incorporating citral essential oil. *J. Food Drug Anal.* 30, 1–8.
- Maali, A., Mosavian, M.H., 2013. Preparation and application of nanoemulsions in the last decade (2000–2010). *J. Dispers. Sci. Technol.* 34, 92–105.
- Mathews, G., 2008. *Pesticide Application Methods*, third ed. John Wiley & Sons, p. 431.
- McClements, D.J., 2004. *Food Emulsions: Principles, Practices, and Techniques*. CRC Press.
- McClements, D.J., 2012. Nanoemulsions versus microemulsions: terminology, differences, and similarities. *Soft Matter* 8 (6), 1719–1729.
- Mishra, R.K., Soni, G.C., Mishra, R.P., 2014. A review article: on nanoemulsion. *World J. Pharm. Sci.* 3, 258–274.
- Mou, D., Chen, H., Du, D., Mao, C., Wan, J., Xu, H., Yang, X., 2008. Hydrogel-thickened nanoemulsion system for topical delivery of lipophilic drugs. *Int. J. Pharm.* 353, 270–276.
- Nunes, C.A., 2012. Biological control of postharvest diseases of fruit. *Eur. J. Plant Pathol.* 133, 181–196.
- Oliveira, E.C.V., Boock, K.P., Maruno, M., Rocha-Filho, P.A., 2011. Accelerated stability and moisturizing capacity of emulsions presenting lamellar gel phase obtained from Brazilian natural raw material. *J. Dispers. Sci. Technol.* 32, 1135–1139.
- Parvu, M., Parvu, A.E., 2011. Antifungal plant extracts. In: *Science Against Microbial Pathogens: Communicating Current Research and Technological Advances*. Formatex Research Center, Badajoz, Spain, pp. 1055–1062.
- Parvu, M., Parvu, A.E., Craciun, C., Barbu-Tudoran, L., Tamaş, M., 2008. Antifungal activities of *Chelidonium majus* extract on *Botrytis cinerea* in vitro and ultrastructural changes in its conidia. *J. Phytopathol.* 156, 550–552.
- Parvu, M., Parvu, A.E., Craciun, C., Barbu-Tudoran, L., Vlase, L., Tamas, M., Molnar, A.M., 2010. Changes in *Botrytis cinerea* conidia caused by *Berberis vulgaris* extract. *Not. Bot. Horti. Agrobi.* 38, 15–20.
- Rao, J., McClements, D.J., 2012. Lemon oil solubilization in mixed surfactant solutions: rationalizing microemulsion and nanoemulsion formation. *Food Hydrocoll.* 26, 268–276.
- Reynolds, E.S., 1963. The use of lead citrate at high pH as an electron-opaque stain in electron microscopy. *J. Cell Biol.* 17, 208–212.
- Ribeiro, R.C.D.A., Barreto, S.M.A.G., Ostrosky, E.A., Rocha-Filho, P.A.D., Veríssimo, L.M., Ferrari, M., 2015. Production and characterization of cosmetic nanoemulsions containing *Opuntia ficus-indica* (L.) mill extract as moisturizing agent. *Molecule* 20, 2492–2509.
- Sasidharan, S., Ping, K.Y., Latha, L.Y., Lachumy, S.J., 2012. *Screening Methods in the Study of Fungicidal Property of Medicinal Plants*. INTECH Open Access Publisher.
- Shafiq, S., Shakeel, F., Talegaonkar, S., Ahmad, F.J., Khar, R.K., Ali, M., 2007. Development and bioavailability assessment of ramipril nanoemulsion formulations. *Eur. J. Pharm. Biopharm.* 66, 227–243.
- Solans, C., Izquierdo, P., Nolla, J., Azemar, N., Garcia-Celma, M.J., 2005. Nano-emulsions. *Curr. Opin. Colloid Interface Sci.* 10, 102–110.
- Stangarlin, J.R., Kuhn, O.J., Assi, L., Schwan-Estrada, K.R.F., 2011. Control of plant diseases using extracts from medicinal plants and fungi. In: *Science Against Microbial Pathogens: Communicating Current Research and Technological Advances*. vol. 2. Formatex, Badajoz, pp. 1033–1042.
- Sugumar, S., Clarke, S.K., Nirmala, M.J., Tyagi, B.K., Mukherjee, A., Chnadrasekaran, N., 2014. Nanoemulsion of eucalyptus oil and its larvicidal activity against *Culex quinquefasciatus*. *Bull. Entomol. Res.* 104, 393–402.
- Surassmo, S., Srinuanchai, W., Yostawonkul, J., Ruktanonchai, U., 2013. Formulation development of plai nanoemulsion based on the influence of surfactant combinations. *Chiang Mai J. Sci.* 40, 994–999.
- Tadros, T.F., Vandamme, A., Leveck, B., Booten, K., Stevens, C.V., 2004. Stabilization of emulsions using polymeric surfactants based on inulin. *Adv. Colloid Interface Sci.* 108, 207–226.
- Taiga, A., Suleiman, M.N.W., Olufolaji, D.B., 2008. Comparative in vitro inhibitory effects of cold extracts of some fungicidal plants on *Fusarium oxysporium* mycelium. *Afr. J. Biotechnol.* 7, 3306–3308.
- Tamilvanan, S., 2009. Formulation of multifunctional oil-in-water nanosized emulsions for active and passive targeting of drugs to otherwise inaccessible internal organs of the human body. *Int. J. Pharm.* 381, 62–76.
- Trotta, M., Gallarate, M., Pattarino, F., Carlotti, M.E., 1999. Investigation of the phase behaviour of systems containing lecithin and 2-acyl lysolecithin derivatives. *Int. J. Pharm.* 190, 83–89.

- Veerakumar, K., Govindarajan, M., Rajeswary, M., Muthukumaran, U., 2014. Low-cost and eco-friendly green synthesis of silver nanoparticles using *Feronia elephantum* (Rutaceae) against *Culex quinquefasciatus*, *Anopheles stephensi*, and *Aedes aegypti* (Diptera: Culicidae). *Parasitol. Res.* 113, 1775–1785.
- Verma, V.C., Kharwar, R.N., Gange, A.C., 2010. Biosynthesis of antimicrobial silver nanoparticles by the endophytic fungus *Aspergillus clavatus*. *Nanomedicine* 5 (1), 33–40.
- Vior, M.C.G., Monteagudo, E., Dicio, L.E., Awruch, J.A., 2011. comparative study of a novel lipophilic phthalocyanine incorporated into nanoemulsion formulations: photophysics, size, solubility and thermodynamic stability. *Dyes Pigm.* 91, 208–214.
- Wang, L., Li, X., Zhang, G., Dong, J., Eastoe, J., 2007. Oil-in-water nano-emulsions for pesticide formulations. *J. Colloid Interface Sci.* 314, 230–235.
- Ziedan, E.S.H., Saad, M.M., El-Kafrawy, A.A., Sahab, A.F., Mossa, A.T.H., 2022. Evaluation of essential oils nanoemulsions formulations on *Botrytis cinerea* growth, pathology and grey mould incidence on cucumber fruits. *Bull. Natl Res. Cent.* 46 (1), 1–9.